BIOCHEMISTRY
including biophysical chemistry & molecular biology

Article

pubs.acs.org/biochemistry

Relative and Regional Stabilities of the Hamster, Mouse, Rabbit, and Bovine Prion Proteins toward Urea Unfolding Assessed by Nuclear Magnetic Resonance and Circular Dichroism Spectroscopies

Olivier Julien,[†] Subhrangsu Chatterjee,[†] Trent C. Bjorndahl,[‡] Braden Sweeting,[§,∥] Sandipta Acharya,[‡] Valentyna Semenchenko,[⊥] Avijit Chakrabartty,[§,∥,#] Emil F. Pai,[§,∥] David S. Wishart,[‡,⊥] Brian D. Sykes,*[,†] and Neil R. Cashman[@]

[†]Department of Biochemistry, University of Alberta, Edmonton, AB, Canada T6G 2H7

[‡]Department of Biological Sciences, University of Alberta, Edmonton, AB, Canada T6G 2E8

[§]Department of Medical Biophysics, University of Toronto, Toronto, ON, Canada M5G 2M9

[∥]The Campbell Family Cancer Research Institute, Ontario Cancer Institute, MaRS/TMDT, 101 College Street, Toronto, ON, Canada M5G 1L7

[⊥]National Institute of Nanotechnology (NINT), National Research Council, 11421 Saskatchewan Drive, Edmonton, AB, Canada T6G 2M

[#]Departments of Biochemistry and Molecular Genetics, University of Toronto, Toronto, ON, Canada M5S 1A8

[@]Department of Medicine (Neurology) and Brain Research Centre, University of British Columbia, Vancouver, BC, Canada V6T2B5

Supporting Information

ABSTRACT: The residue-specific urea-induced unfolding patterns of recombinant prion proteins from different species (bovine, rabbit, mouse, and Syrian hamster) were monitored using high-resolution ^{1}H nuclear magnetic resonance (NMR) spectroscopy. Protein constructs of different lengths, and with and without a His tag attached at the N-terminus, were studied. The various species showed different overall sensitivities toward urea denaturation with stabilities in the following order: hamster ≤ mouse < rabbit < bovine protein. This order is in agreement with recent circular dichroism (CD) spectroscopic measurements for several species [Khan, M. Q. (2010) *Proc. Natl. Acad. Sci. U.S.A. 107*, 19808−19813] and for the bovine protein presented herein. The $[urea]_{1/2}$ values determined by CD spectroscopy parallel those of the most stable residues observed by NMR spectroscopy. Neither the longer constructs containing an additional hydrophobic region nor the His tag influenced the stability of the structured domain of the constructs studied. The effect of the S174N mutation in rabbit PrP^C was also investigated. The rank order of the regional stabilities within each protein remained the same for all species. In particular, the residues in the β-sheet region in all four species were more sensitive to urea-induced unfolding than residues in the α2 and α3 helical regions. These observations indicate that the regional specific unfolding pattern is the same for the four mammalian prion proteins studied but militate against the idea that PrP^{Sc} formation is linked with the global stability of PrP^C.

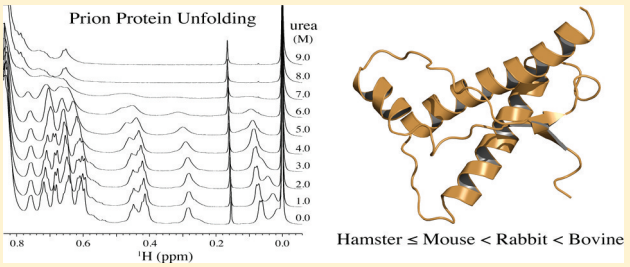

Prion diseases or transmissible spongiform encephalopathies (TSEs) are a group of rare and fatal neurodegenerative disorders that can be sporadic, inherited, or acquired by infectious means. These include Creutzfeldt-Jacob disease (CJD), kuru, familial fatal insomnia (FFI), and Gerstmann-Sträussler-Scheinker syndrome (GSSS) in humans; scrapie in sheep and goats; bovine spongiform encephalopathy (BSE) in cattle; transmissible mink encephalopathy (TME) in mink; chronic wasting disease (CWD) in mule deer and elk; and feline spongiform encephalopathy (FSE) in cats.[1−6] These diseases are associated with a conformational conversion of the normal cellular, membrane-anchored prion protein (PrP^C) into an oligomeric, β-sheet rich, proteinase-K resistant, infectious form termed PrP^{Sc}.[7−9] Within the context of the "protein only" hypothesis, the misfolded prion protein can recruit PrP^C to form oligomeric aggregated structures. Several binding partners for PrP^C have been proposed over the years, like the 37/67 kDa laminin receptor.[10] An unknown protein, "protein X", has also been proposed to bind to the cellular prion protein during prion propagation.[11] The precise biological role of PrP^C is still not known, but roles in signal transduction[12] and regulation of metal metabolism[13] have been suggested. The mature PrP^C

Received: May 10, 2011
Revised: July 28, 2011
Published: July 29, 2011

protein consists of ~210 amino acid residues and is attached to the outer leaflet of the plasma membrane via a C-terminal glycophosphatidylinositol (GPI) anchor. PrP^C has an unstructured flexible N-terminal region (residues 23−126) and a C-terminal folded domain (residues 127−230).[14] Many crystallographic and NMR structures of the C-terminal domains of PrP^C from a wide variety of different species have been determined by several groups. The three-dimensional structures of the folded domain were found to be very similar,[15] all displaying a globular fold consisting of three α-helices (α1−α3) together with a short two-stranded antiparallel β-sheet (β1 and β2). Helices α2 and α3 are linked by a Cys(179)−Cys(214) disulfide bridge in PrP^C. The β1 (residues 127−131) and β2 (residues 161−164) strands are each made of four amino acids. The α1−α3 helices are of different lengths and composed of ~10 (residues 144−154), ~20 (residues 174−194), and ~30 (residues 200−230) amino acids, respectively.

Despite considerable effort, the structure of oligomeric PrP^{Sc} and the mechanism underlying the conversion of PrP^C to the PrP^{Sc} form remain unclear. Convincing evidence that oligomeric PrP^{Sc} consists of more β-sheet rich and less α-helical structures exists, whereas the monomeric noninfectious PrP^C is composed of mostly α-helical components.[7−9] Molecular dynamics simulations suggest that extension of the native antiparallel β-sheet in PrP^C may be the key conformational transition leading to PrP^{Sc}.[16] The same authors proposed a spiral model of the prion protofibril based on this elongation of the native β-sheet of PrP^C.[17] On the other hand, the Prusiner group has proposed different β-helical models over the years to fit the electron microscopic map of two-dimensional (2D) crystals of PrP^{Sc}.[18,19] Ultimately, their studies suggested that the high β-sheet content of PrP^{Sc} forms an assembly of left-handed trimeric β-helices.[19] This trimeric model accommodates the PrP sequence from residues 89−175 in a β-helical conformation with the C-terminus (residues 176−227) retaining the disulfide-linked α-helical conformation observed in the normal cellular isoform. This model requires the dissociation of the native β-sheet of PrP^C for conversion of the protein into PrP^{Sc}. Interestingly, the NMR structure of the yeast prion HET-s recently reported revealed a similar β-solenoid structure.[20] The Surewicz group, on the other hand, obtained contradictory results using site-directed spin labeling and EPR spectroscopy and propose that human prion protein amyloids consist of a parallel in-register β-structure.[21] Recently, they reported that the infectious form of PrP^{Sc} consists of β-strands and short turns, but, most importantly, no α-helices.[22] Nonetheless, a key question that remains unanswered is what leads to these misfolded structures. Using molecular dynamics simulations, a study suggested that the presence of the D178N mutation in PrP^C would destabilize the native β-sheet of PrP^C, making the protein more susceptible to unfolding.[23] Structural destabilization of PrP^C in the D178N mutant would be correlated with the weakening of the hydrogen bonding network involving the mutated residue and the side chains of R164 and Y128, providing a safety mechanism for the "unzipping" of the antiparallel β-sheet in PrP^C.[23] Also, mono- and polyclonal YYR (Tyr-Tyr-Arg) epitope-specific antibodies selectively immunoprecipitated the pathogenic PrP^{Sc} form,[24] consistent with exposure of this motif in β2, which would require a dissociation of the β-sheet. NMR relaxation measurements of mouse PrP(113−231) showed slow conformational fluctuations in the β-sheet of the prion protein.[25] Finally, urea denaturation studies of bovine PrP^C performed in our group suggest that the native β-sheet of PrP^C is not as stable as its helical regions,[26] supporting the idea that the β-sheet dissociation is a required step in the PrP^C to PrP^{Sc} structural conversion.

While prion infection is possible in many animals, some species like chicken, turtle, and rabbit[27−29] seem to be immune to prion infection. Furthermore, a "species barrier" exists in which prions from one species do not readily cross to another prion-infectable species. Evidence indicates that the species barrier is largely controlled by the primary sequence of PrP. In early work, Priola and Chesebro used mouse prions to infect mouse neuroblastoma cells expressing recombinant mouse or hamster PrP.[30] They showed that the mouse PrP, but not the hamster PrP, could be seeded by mouse prion and that a single hamster-specific amino acid, M139, inhibited the conversion. The sequences of hamster and mouse PrPs are 94% identical, with only three residues different within the amyloidogenic sequence (residues 90−145). Hamster PrP has three Met residues at positions 109, 112, and 139, while mouse PrP has Leu, Val, and Ile at those positions, respectively. However, more evidence supporting the possibility of crossing this species barrier continues to emerge.[31] For example, the formerly defined species barrier of CWD between deer and humans may not be hard to overcome as previously thought.[32]

In this study, we investigate whether a species difference leads to a different region-specific unfolding pattern of the prion protein. We use ^{1}H NMR spectroscopy to monitor the residue-specific urea-induced unfolding of prion proteins from four different mammalian species: (i) bovine, (ii) rabbit, (iii) mouse, and (iv) Syrian hamster. We previously studied the initial phases of PrP^C protein unfolding induced by urea to help unravel the mechanism of PrP structural conversion.[26] The rationale is that urea-induced denaturation of PrP^C can generate non-native, partially unfolded PrP structures that may serve as efficient substrates for amyloid fibrils. Baskakov et al. demonstrated the conversion of recombinant human PrP(90−231) to amyloid fibrils in the presence of urea; these fibrils possess an epitope presentation similar to that of PrP^{Sc}, suggesting a common overall architecture.[33] A study of the kinetics of amyloidogenesis, starting from the β-oligomer of mouse PrP(89−231), showed a decrease in the β-oligomeric population coincided with an increase in the α-helical rich PrP population, suggesting that amyloid fibrils can be formed directly from PrP^C in the presence of urea as a denaturant.[34] The ultimate goal of this study is to correlate the global and region-specific stability of PrP^C from four mammalian species to their respective susceptibilities in developing prion diseases.

MATERIALS AND METHODS

Protein Purification. The sequences of the PrP protein constructs used in this study are shown aligned in Figure 1. The C-terminal domain of the bovine prion protein [designated bPrP(121−230)] was expressed and purified in *Escherichia coli* as previously described, based on a methodology developed for human PrP.[35] Synthetic genes corresponding to residues 90−232 of the Syrian hamster prion [designated shPrP(90−232)] and residues 120−232 of the Syrian hamster prion [designated shPrP(120−232H)] as well as a synthetic gene corresponding to residues 90−232 of the mouse prion [designated moPrP(90−232)] were designed using codons optimized for *E. coli* expression and synthesized by DNA 2.0 (Menlo Park,

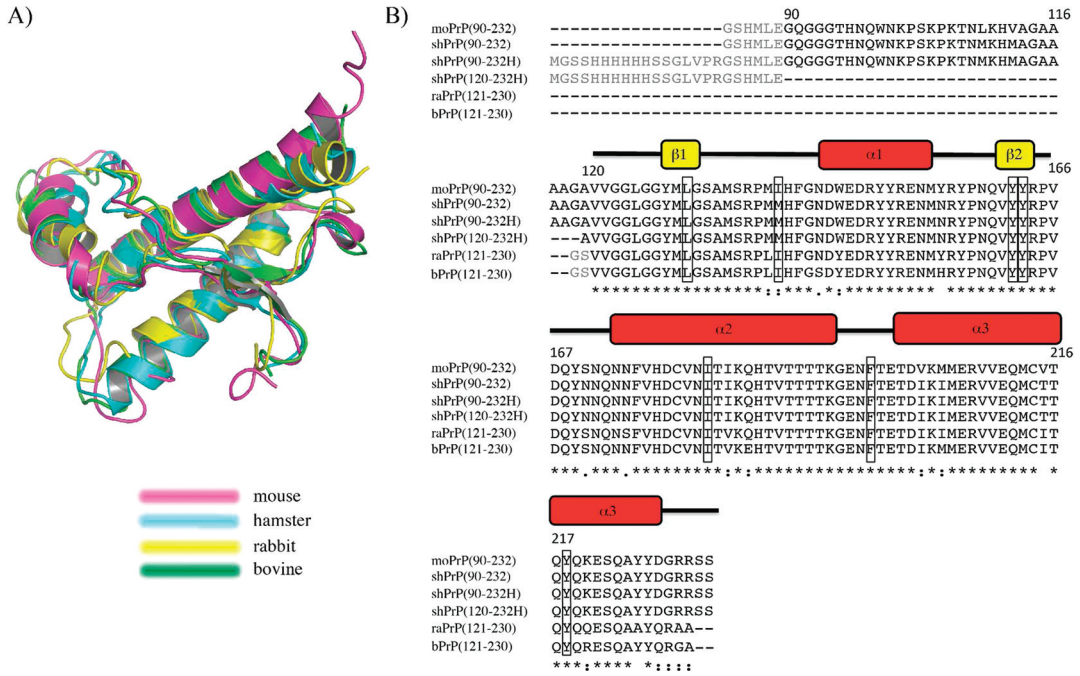

Figure 1. Primary sequence alignment and three-dimensional structure superimposition of mammalian prion proteins. (A) Superimposition of the structures of the C-terminal domains of bovine (PDB entry 1DWY), hamster (PDB entry 1B10), mouse (PDB entry 1XYX), and rabbit (PDB entry 2FJ3) PrP^C. (B) Sequence alignment of the bovine, hamster, mouse, and rabbit constructs used in this study. The amino acids colored gray are from the His tag or leftover from cleavage, and the ones highlighted with a box indicate the residues monitored by one-dimensional ^1H NMR in this study.

CA). Each gene included a 22-residue N-terminal fusion tag containing six His residues and an enterokinase cleavage site (MGSSHHHHHHSSGLVPRGSHML). Each gene was cloned into a separate pET15b expression vector between *Xho*I and *Eco*RI restriction sites and heat shock transformed into *E. coli* strain BL21(DE3). The DNA sequence encoding rabbit PrP(121−230) was cloned using the pET28a system (Novagen, Gibbstown, NJ) and expressed with an N-terminal six-His tag and a thrombin protease cleavage site. The constructs originated from three different groups, which explains the differences in length. Prior to use, all of the proteins were dialyzed against a 10 mM ammonium bicarbonate buffer (pH 8.5) for at least 3 days and then lyophilized. The purity of the protein was verified using NMR and mass spectrometry. We used NMR to confirm the presence or absence of Tris, acetate, glutathione, and salt from the buffers used in the purification (concentration of salt determined by comparison of pulse lengths between samples).

NMR Samples. All the NMR samples for prion proteins from four different species were prepared with 2−5 mg of prion protein in 500−550 μL of NMR buffer containing 10 mM $NaC_2H_3O_2$, 0.3 mM deuterated 2,2-dimethyl-2-silapentane-5-sulfonic acid (DSS-d_6), and 0.012% (w/v) NaN_3 in D_2O. The pH values of the samples were in the range of 5.7−7.2 according to the chemical shift of the acetate methyl group based on a previously described methodology.[36] Regardless of the initial pH of the NMR sample, the addition of 1 M urea (first step of the titration) buffered the pH to approximately 5.7 in all samples (under the experimental conditions used in this studies). The initial pH values were slightly different to help to dissolve PrP^C, because the different constructs had slightly different properties. The urea-induced unfolding of bovine, hamster, mouse, and rabbit PrP^C of different lengths was performed by adding solid deuterated urea (urea-d_4, Sigma-Aldrich) directly to the NMR tube. The urea concentration was increased by 1 M at each titration step until the concentration reached 9 M. The protein and urea concentrations were corrected for the partial specific volume of the added urea.

NMR Spectroscopy. The one-dimensional (1D) ^1H NMR experiments were all performed on a 600 and 800 MHz Varian INOVA NMR spectrometer. The 1D ^1H NMR spectra were acquired with 256 transients, a spectral width of 14.0 ppm, a relaxation delay of 2.0 s, and an acquisition time of 3.0 s. For all spectra, water and urea were both presaturated using the multiple-frequency presaturation feature of VnmrJ (2.2D) BioPack (Varian, Inc.). Processing of the 1D spectra was performed with VnmrJ version 2.1B (Varian, Inc.) using a line broadening of 1.5 Hz. The vertical and integral scales were adjusted according to the dilution of the protein caused by the addition of solid urea. We analyzed the data using different methods: peak intensity, peak integral, and peak deconvolution. All three methods are consistent with one another, but the peak integral or peak deconvolution approaches take into account the effect of line broadening in the spectra, the latter being more reliable when peak overlap is present. Accordingly, the peak integrals of different isolated resonances were calculated by the deconvolution method in a window of approximately 0.1−0.2 ppm, applying a drift correction on the baseline. The peak integral of a given resonance was normalized to the first titration point (at 0 M urea) and plotted versus increasing urea concentrations (0−9 M).

Circular Dichroism Spectroscopy. Lyophilized bPrP(121−230) protein was reconstituted in 9 M urea buffer [50 mM $NaC_2H_3O_2$, 70 mM NaCl, and 9 M urea (pH 7.0)] and diluted into the same buffer without urea to provide 28 samples with varying concentrations of urea (from 1 to 9 M) with a final protein concentration of ~0.5 mg/mL. Additionally, a second sample devoid of NaCl was prepared in the same

dx.doi.org/10.1021/bi200731e | *Biochemistry* 2011, 50, 7536−7545

manner in 8.2 M urea buffer [20 mM $KNaHPO_4$ and 8.2 M urea (pH 7)] and diluted into the same buffer providing 30 samples with a final protein concentration of ~1 mg/mL. The protein samples were allowed to equilibrate for 4 days at 25 °C prior to data acquisition. All CD spectra were recorded in the far-UV region (212−260 nm) at 25 °C in a 0.02 cm path length quartz cell on an Olis DSM 17 spectropolarimeter. CD spectra were averaged over five individual scans using a bandwidth of 1 nm. The CD spectra were smoothed with a 5 nm window. Following the collection of CD data, the absorbance at 280 nm was recorded on an ND-1000 nanodrop UV spectrometer, and an extinction coefficient of 16515 M^{-1} cm^{-1} was used to calculate the final protein concentrations of each sample prior to the calculation of molar ellipticity values. The normalized CD values at 220 and 229 nm were used to calculate the fraction folded (f_{folded}) at each wavelength using the method described by Khan et al.[37]

Data Analysis. The data were analyzed assuming a two-state transition for the protein denaturation, and a free energy of unfolding (ΔG_{F-U}) linearly dependent on the concentration of denaturant:[38,39]

$$\Delta G_{F-U} = \Delta G^0_{F-U} - m[\text{urea}] \quad (1)$$

where m is the sensitivity toward urea unfolding, ΔG^0_{F-U} is the Gibbs free energy of unfolding in the absence of denaturant, and [urea] is the concentration of denaturant. The fraction of the folded form (f_{folded}) is then represented as

$$f_{folded} = \frac{1}{1 + e^{(-\Delta G^0_{F-U} + m[\text{urea}])/RT}} \quad (2)$$

when the fraction of the folded form of the protein is 50%:

$$\Delta G^0_{F-U} = m[\text{urea}]_{1/2} \quad (3)$$

This leads to the following formula for fitting the data to directly extract the thermodynamic properties of the protein upon denaturant-induced unfolding:

$$\frac{I}{I_0} = \frac{a}{1 + e^{m([\text{urea}]-[\text{urea}]_{1/2})/RT}} \quad (4)$$

where I is the peak integral at a given urea concentration, I_0 is the peak integral at 0 M urea, [urea] is the concentration of urea, $[\text{urea}]_{1/2}$ is the concentration of urea required to decrease the peak integral by half, a is a scaling constant, R is the gas constant, and T is the temperature.

RESULTS

We used high-resolution ^{1}H nuclear magnetic resonance spectroscopy to study the unfolding of recombinant prion proteins from four different species, i.e., bovine, hamster, mouse, and rabbit. The primary structure alignment of these proteins shown in Figure 1 reflects the high level of sequence identity of PrP^C. In addition, the three-dimensional structures of the C-terminal regions of these proteins have been previously determined by NMR spectroscopy, and their structures were found to be practically identical (PDB entries 1DWZ for bovine, 1B10 for hamster, 1XYX for mouse, and 2FJ3 for rabbit). The focus of this study is to compare the urea-induced unfolding transition of different residues at different sites in each of the four prion proteins, to determine if the stability of any of these regions can be correlated with the susceptibility of each species to develop prion diseases (i.e., rabbit not disposed to developing TSEs). PrP constructs of different lengths and from different species were used in this study, including moPrP(90−232), shPrP(90−232H), shPrP(90−232), shPrP(120−232H), bPrP(121−230), and raPrP(121−230). For the sake of consistency, the sequence numbering used herein to describe the different species was adjusted to match that of the bovine sequence. The hamster constructs of three different lengths were studied to investigate the impact of the hydrophobic region (residues 90−120) on the well-stabilized folded region (residues 121−230), and of the effect of the presence or absence of the His tag used for protein purification. The effect of the S174N mutation in raPrP(121−230) was also studied. It has previously been shown that the 1D ^{1}H NMR spectrum of recombinant bPrP(121−230) is virtually identical to the spectrum of bPrP(23−230) isolated from healthy calf brains,[40] justifying the use of recombinant PrPs in our study.

The ^{1}H NMR spectra of these prion proteins were recorded using D_2O as a solvent to detect the β-sheet Hα and aromatic proton NMR signals, which would otherwise be buried under strong water and amide proton signals, respectively. Addition of urea to the protein induces unfolding monitored by different residues at different positions in the prion proteins. The various residues showed a different order of disappearance of their proton peaks in the NMR spectra with increasing concentrations of urea. We choose well-isolated resonances in the 1D NMR spectra (L130 Hδ2, I139 Hδ1, I182 Hγ2, I182 Hδ1, F198 Hα, Y162 Hα, Y218 Hδ, and Y163 Hδ) conveniently located in different regions throughout the structure of PrP^C (β1, α2, loop, β2, and α3) to study the region-specific unfolding. These resonances showed minimum overlap with other resonances so that they could be accurately integrated and were previously shown to exhibit slow conformational exchange on the order of 1 s^{-1}.[26] The later fact justifies the use of the peak integral for the analysis to reflect the concentrations of folded and unfolded species. Stacked plots of the 1D ^{1}H spectra acquired during each urea-induced denaturation experiment for each species are presented in Figure 2 (see Figure S1 of the Supporting Information for the comparison of the different shPrP constructs and Figure S2 of the Supporting Information for comparison of the wild-type and S174N rabbit constructs). For all spectra presented, the vertical scales were corrected for the volume increase (i.e., dilution factor) caused by the addition of urea (see Materials and Methods). The peak integral of each resonance is presented in Figure S3 of the Supporting Information as a function of urea concentration. Because each resonance followed a sigmoidal denaturation profile characteristic of a two-state mechanism of unfolding, the peak integrals were fit using eq 4. Two thermodynamic parameters were extracted for each residue: $[\text{urea}]_{1/2}$, the urea concentration at the midpoint of unfolding, and m, the slope of the denaturation profile, which is representative of the sensitivity of each resonance upon urea-induced unfolding. The $[\text{urea}]_{1/2}$ values are listed in Table 1, while the ΔG_{F-U} and m values are listed in Table 2.

We observed that bPrP(121−230) has a higher resistance toward urea-induced unfolding compared to hamster, mouse, and rabbit prion protein constructs (Figure 1). For example, $[\text{urea}]_{1/2}$ for I182 Hγ2 of bPrP(121−230) equals 7.1 ± 0.1 M compared to 5.2 ± 0.1 M for shPrP(120−232), 4.9 ± 0.2 M for moPrP(90−232), and 6.1 ± 0.1 M for raPrP(121−230)

dx.doi.org/10.1021/bi200731e | Biochemistry 2011, 50, 7536−7545

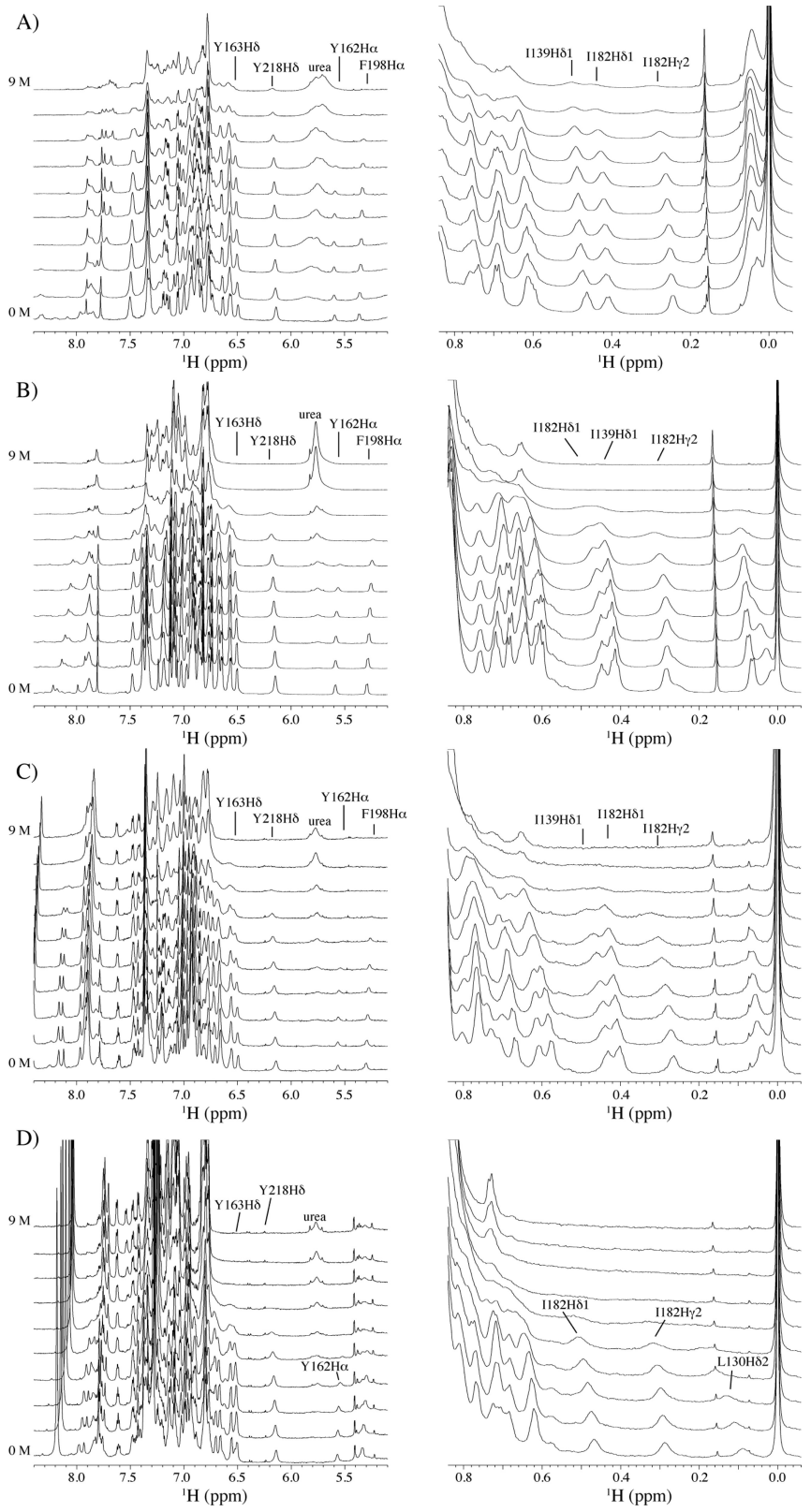

Figure 2. Stacked plots as a function of urea concentration (0−9 M) of two regions of the 1D ^{1}H NMR spectra for (A) bPrP(121−230), (B) raPrP(121−230), (C) moPrP(90−232), and (D) shPrP(90−232). The left panels show the aromatic and α-proton resonances, while the right panels show the upfield-shifted methyl resonances for each protein. The spectra were all acquired at 800 MHz.

(see Table 1). As previously observed for bPrP(121−230),[26] residues located in the β-sheet of PrP^C for all species (i.e., L130 Hδ2 located in β1 and Y162 Hα and Y163 Hδ located in β2) have lower $[\text{urea}]_{1/2}$ values compared to those of other protons located in other regions of the proteins. Within all six different protein constructs from four different species, two groups of

dx.doi.org/10.1021/bi200731e | *Biochemistry* 2011, 50, 7536−7545

Table 1. $[urea]_{1/2}$ Values Measured for Different ^1H Resonances in Various PrP^C Constructs

species	construct	$[urea]_{1/2}$								average $[urea]_{1/2}$
		I182 Hδ1	I182 Hγ2	L130 Hδ2	I139 Hδ1	F198 Hα	Y162 Hα	Y163 Hδ	Y218 Hδ	
mouse	moPrP(90−232)	5.5 ± 0.2	4.9 ± 0.2	–	4.6 ± 0.1	5.1 ± 0.1	3.8 ± 0.3	3.0 ± 0.3	5.5 ± 0.1	4.6
hamster	shPrP(90−232H)	4.9 ± 0.3	5.1 ± 0.1	4.4 ± 0.1	–	4.1 ± 0.2	2.8 ± 0.2	–	5.0 ± 0.1	3.7
	shPrP(90−232)	4.0 ± 0.1	4.3 ± 0.1	3.8 ± 0.1	–	–	3.6 ± 0.1	4.5 ± 0.3	5.0 ± 0.1	4.2
	shPrP(120−232H)	5.6 ± 0.1	5.2 ± 0.1	3.9 ± 0.1	–	4.5 ± 0.2	3.3 ± 0.5	3.5 ± 0.5	5.4 ± 0.1	4.5
rabbit	raPrP(121−230)	6.6 ± 0.1	6.1 ± 0.1	–	6.8 ± 0.2	5.3 ± 0.1	4.0 ± 0.3	6.3 ± 0.2	6.9 ± 0.2	6.0
bovine	bPrP(121−230)	7.3 ± 0.1	7.1 ± 0.1	–	7.7 ± 0.3	7.2 ± 0.1	5.4 ± 0.1	6.2 ± 0.2	7.6 ± 0.1	6.9

resonances showed a consistent difference in sensitivity order toward urea-induced unfolding; residues in helices α2 and α3 and those in loop regions showed higher $[urea]_{1/2}$ values, whereas protons from residues in the β-sheet region showed lower $[urea]_{1/2}$ values (Figure 3). For instance, $[urea]_{1/2}$ values of Y162 Hα are 5.4 ± 0.1 M in bPrP(121−230), 3.3 ± 0.5 M in shPrP(120−232), 3.8 ± 0.2 M in moPrP(90−232), and 4.0 ± 0.3 M in raPrP(121−230). These relatively low $[urea]_{1/2}$ values (compared to that of I182 Hγ2, for example) suggest that the initial stages of unfolding and misfolding occur in the β-sheet region for the four different mammalian prion proteins. Residues from the α2 and α3 regions (i.e., I182 Hγ2, I182 Hδ1, and Y218 Hδ) were found to have higher $[urea]_{1/2}$ values, suggesting a certain resistance toward urea unfolding. The hydrophobic interaction between both α-helices is likely to be responsible for this increased stability.[26,41] Our results are agreement with the "banana peeling" PrP misfolding mechanism proposed by Adrovel et al.,[42] showing a very stable interaction between helices α2 and α3 (see Discussion and Conclusion). As a control, neither the presence of a His tag nor the addition of the hydrophobic region resulted in negligible differences in the denaturation profiles of $shPrP^C$ (Figure S1 of the Supporting Information). The stacked plots of the 1D ^1H NMR spectra of the three constructs of $shPrP^C$ of different lengths [shPrP(90−232), shPrP(90−232H), and shPrP(120−232H)] showed a high level of similarity.

Among the four types of mammalian prion proteins, shPrP(90−232) and moPrP(90−232) constructs show a similar overall sensitivity toward urea-induced unfolding. Both are denatured at low urea concentrations compared to $raPrP^C$ and $bPrP^C$, with $moPrP^C$ being slightly more stable than $shPrP^C$. The $[urea]_{1/2}$ values of I182 Hδ1 and I182 Hγ2 for moPrP(90−232) are higher (5.5 ± 0.2 and 4.9 ± 0.2 M, respectively), while those of shPrP(90−232) are 4.0 ± 0.1 and 4.3 ± 0.1 M, respectively. On the other hand, moPrP(90−232) has a lower $[urea]_{1/2}$ of 3.0 ± 0.3 M for Y163 Hδ, in comparison to a value of 4.5 ± 0.3 M for shPrP(90−232). The resonances of rabbit PrP^C all have higher $[urea]_{1/2}$ values compared to those of $shPrP^C$ and $moPrP^C$, indicating a higher resistance toward urea denaturation. Some protons such as I182 Hδ1, I182 Hγ2, I139 Hδ1, and Y218 Hδ in rabbit PrP^C even show sensitivity similar to those of resonances in $bPrP^C$, but protons such as F198 Hα and Y162 Hα show lower sensitivity toward urea denaturation as found in $shPrP^C$ and $moPrP^C$ (see Table 1). If one globally compares the $[urea]_{1/2}$ values of these mammalian prion proteins, the relative order of stability toward urea-induced denaturation is as follows: hamster ≤ mouse < rabbit < bovine. A bar graph of the regional $[urea]_{1/2}$ values measured from the different proton resonances for the different PrP^C constructs from four different species is presented in Figure 4.

The stability of the loop (residues 166−175) in PrP^C has been thought for a long time to be an important factor in the PrP^C to PrP^{Sc} conversion.[43,44] The N174S mutation in mouse PrP^C, for example, which mimics the sequence found in rabbit PrP^C, can induce resistance to PrP^{Sc} conversion.[29] Inversely, one could think that the reversed S174N mutation in rabbit PrP^C (sometimes termed S173N in the literature, depending on the nomenclature used) could lead to a destabilization of the protein structure. Therefore, we have investigated the effect of the S174N mutation in $raPrP^C$ using 1D ^1H NMR and the

dx.doi.org/10.1021/bi200731e | Biochemistry 2011, 50, 7536−7545

Table 2. ΔG^0_{F-U} and m Values Measured for Different ^{1}H Resonances in Different PrP^C Constructs

PrP construct	I182 Hδ1	I182 Hγ2	L130 Hδ2	I139 Hδ1	F198 Hα	Y162 Hα	I163 Hδ	Y218 Hδ
				ΔG^0_{F-U} (kJ mol^{-1})				
moPrP(90−232)	32.8 ± 8.1	17.1 ± 4.6	–	32.8 ± 10.5	13.7 ± 3.6	8.2 ± 2.0	4.8 ± 0.9	41.1 ± 9.7
shPrP(90−232H)	9.6 ± 2.8	18.0 ± 2.1	15.1 ± 2.5	–	9.4 ± 1.6	11.0 ± 4.0	–	19.0 ± 1.8
shPrP(90−232)	17.3 ± 3.2	33.9 ± 5.9	21.5 ± 3.4	–	–	25.5 ± 4.7	13.3 ± 3.3	60.0 ± 8.9
shPrP(120−232H)	31.7 ± 3.7	16.9 ± 2.4	20.2 ± 2.8	–	22.4 ± 8.9	8.7 ± 3.9	7.6 ± 3.0	20.0 ± 3.0
raPrP(121−230)	27.6 ± 3.5	19.0 ± 2.0	–	17.7 ± 4.0	21.8 ± 1.9	9.2 ± 3.0	14.8 ± 3.7	17.6 ± 2.9
bPrP(121−230)	18.8 ± 1.9	13.7 ± 5.2	–	19.1 ± 1.1	21.8 ± 4.3	26.7 ± 2.0	24.1 ± 3.5	15.9 ± 2.1
				m (kJ mol^{-1} M^{-1})				
moPrP(90−232)	6.0 ± 1.6	3.5 ± 0.8	–	7.4 ± 2.1	2.7 ± 0.5	2.2 ± 0.4	1.6 ± 0.2	7.5 ± 1.6
shPrP(90−232H)	2.0 ± 0.4	3.5 ± 0.6	3.4 ± 0.5	–	2.3 ± 0.3	4.0 ± 1.1	–	3.8 ± 0.3
shPrP(90−232)	4.3 ± 0.7	7.9 ± 1.3	5.7 ± 0.8	–	–	7.1 ± 1.1	3.0 ± 0.6	12.0 ± 1.8
shPrP(120−232H)	5.7 ± 0.6	3.2 ± 0.4	5.2 ± 0.6	–	5.0 ± 1.7	2.6 ± 0.7	2.2 ± 0.6	5.4 ± 0.5
raPrP(121−230)	4.2 ± 0.6	3.1 ± 0.3	–	2.6 ± 0.5	2.7 ± 0.5	2.3 ± 0.6	2.4 ± 0.6	2.5 ± 0.4
bPrP(121−230)	2.6 ± 0.2	1.9 ± 0.7	–	2.5 ± 0.1	3.0 ± 0.5	4.9 ± 0.3	3.9 ± 0.4	2.1 ± 0.3

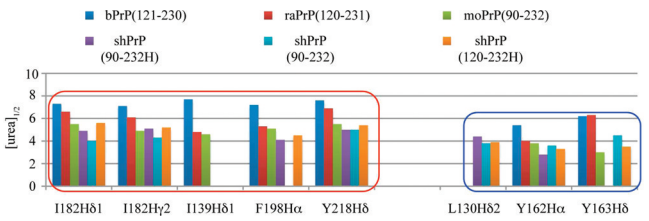

Figure 3. Rank order of the regional stabilities ($[urea]_{1/2}$ values determined by ^{1}H NMR) for bovine, rabbit, mouse, and hamster PrP^C. Residues in the β-sheet region (right) are more sensitive to denaturation than residues found in other regions in the protein (left).

same methodology presented above. The spectra acquired for both proteins revealed an exceptionally nice chemical shift dispersion and strong signal intensity. However, the comparison of the 1D ^{1}H NMR spectra (Figure S3 of the Supporting Information), as well as the 2D NOESY spectra (data not shown), did not show any significant difference between both proteins, at any urea concentration. On one hand, this could indicate that the S174N mutation does not significantly affect the stability of PrP^C and that the global stability of the protein might not be the key to understanding the effect of this mutation (and possibly others) on infectivity. It is also possible that the S174N mutation creates a small regional destabilization surrounding residue 174 that went undetected using this denaturation technique. On a positive note, these results clearly show the reproducibility of the methodology and results presented herein for the other species.

Recently, Khan et al. reported the urea-induced thermodynamic data of hamster, mouse, and rabbit PrP^C using CD spectroscopy. We could not find the thermodynamic characterization of bPrP^C using this technique in the literature. Accordingly, we monitored the urea-induced unfolding of bPrP(121−230) at pH 7 using CD spectroscopy using the same experimental procedures that were used by Khan et al. The fraction folded as a function of urea concentration is presented in Figure S4 of the Supporting Information. We measured a $[urea]_{1/2}$ value of 7.0 M in the presence of low salt (20 mM $KNaHPO_4$) and a slightly lower value of 6.5 M at a higher salt concentration (50 mM $NaC_2H_3O_2$ and 70 mM NaCl). The lower $[urea]_{1/2}$ value measured in the presence of a higher salt concentration is consistent with studies showing that polyanions facilitate PrP conversion and promote de novo prion formation.[45,46]

DISCUSSION AND CONCLUSION

In this study, the NMR-monitored region-specific urea-induced unfolding of PrP^C from bovine, rabbit, mouse, and hamster proteins has been investigated. All species have very similar 1D ^{1}H NMR spectra as expected from their high level of sequence similarity and structural conservation. These include shPrP^C of different lengths and constructs with and without the His tag used for protein purification. Overall, our results indicate that the different protein lengths or the presence of the His tag on the N-terminus of the prion proteins has no influence on stability.

In our previous study, we used 1D ^{1}H and 2D ^{1}H−^{1}H NOESY NMR experiments and showed that the β-sheet region of bPrP(121−230) is more labile in the presence of urea, whereas the α2 and α3 helices are more resistant toward urea-induced unfolding.[26] A theoretical simulation of flexibility versus residue number for human PrP(121−230) also supports a similar pattern of unfolding.[47,48] Within all constructs studied here, residues located in helices α2 and α3 consistently showed a significant resistance against urea unfolding (protons with higher $[urea]_{1/2}$ values) compared to residues located in loops or in the β-sheet region showing lower $[urea]_{1/2}$ values (Figure 3). Our results are in perfect agreement with the banana peeling PrP misfolding mechanism proposed by Adrovel et al.,[42] where the unfolding process would start with the "pealing off" (like a banana) of the interactions between helices α2 α3 and the rest of the globular domain, exposing the highly fibrillogenic seeding element α2−α3. By determining the NMR structure of PrP comprising the hairpin formed by helices α2 and α3, the authors showed that this construct is a stable independently folded unit that would be the aggregation seed that needs to be first exposed to promote conversion from a helical to a β-sheet rich structure.[42]

The bar graph of the $[urea]_{1/2}$ values presented in Figure 4 shows that the relative species stabilities are in the following order: hamster ≤ mouse < rabbit < bovine. For example, if the individual $[urea]_{1/2}$ values are averaged for each species (avg. $[urea]_{1/2}$), these values would represent the average unfolding propensity of all different regions in the protein using NMR spectroscopy. The avg.$[urea]_{1/2}$ values for hamster, mouse,

dx.doi.org/10.1021/bi200731e | Biochemistry 2011, 50, 7536−7545

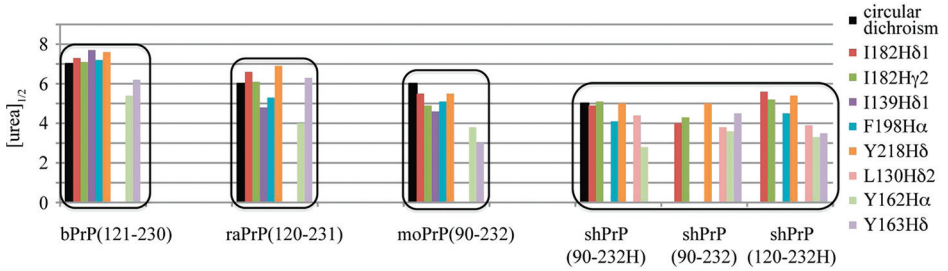

Figure 4. Rank order of the stability toward urea denaturation of the mammalian prion proteins studied. Bar plots represent regional $[urea]_{1/2}$ values monitored using different proton resonances in the ^1H NMR spectrum and the global $[urea]_{1/2}$ value monitored using CD spectroscopy for bovine, rabbit, mouse, and hamster PrPs of different lengths. The CD data for hamster, mouse, and rabbit were taken from ref 37. The rank order of sensitivity toward urea-induced unfolding of the four different species is as follows: hamster ≤ mouse < rabbit < bovine.

rabbit, and bovine are 4.1, 4.6, 6.0, and 6.9 M, respectively. One can also notice that the global $[urea]_{1/2}$ values obtained by Khan et al.,[37] and the complementary data presented for $bPrP^C$ in Figure S4, of the Supporting Information are comparable to those of the most resistant residues observed by NMR spectroscopy (Figure 4). The $[urea]_{1/2}$ values from the CD data represent the global unfolding of the secondary structures of the protein, whereas the $[urea]_{1/2}$ values measured by NMR are specific for residues that are located at different sites in the protein, reflecting the region-specific local unfolding of the molecule. These results indicate that the structural environment of the individual residues forming an α-helix can be perturbed before the perturbation of the secondary structure is observed. However, both methods report the global consequences of denaturants averaged over all the molecules present in the sample but cannot report the unfolding mechanism of single molecules. Overall, the CD spectroscopy measurements agree with the stability ranking of the four mammalian PrP^C forms as seen by NMR (i.e., $shPrP^C$ < $moPrP^C$ < $raPrP^C$ < $bPrP^C$). Of special interest is the fact that bovine PrP^C was found to be the most resistant protein upon urea denaturation, followed closely by rabbit PrP^C. This seems counterintuitive, because rabbits have been shown so far to be immune to prion diseases, while the worldwide outbreak of BSE requires no introduction. Therefore, our results militate against the idea that PrP^{Sc} formation is linked with the global stability of PrP^C.

In addition to this, we have investigated the effect of the S174N mutation in rabbit PrP^C. The mutation was found to have no significant consequence on the stability of PrP^C for the selected residues monitored using NMR. This substitution has been previously suggested to be a destabilizing mutation in PrP^C.[49,50] More specifically, Wen et al. recently reported $[urea]_{1/2}$ values of 6.49 and 6.09 for wild-type and S174N $raPrP^C$, respectively, using CD spectroscopy. On one hand, our results are consistent with these data, showing that wild-type and S174N $raPrP^C$ have a $[urea]_{1/2}$ value close to 6 M. However, we did not observe a significant difference in stability between the proteins. Although our results suggest that the S174N mutation does not significantly affect the overall stability of PrP^C, it is also possible that the S174N mutation creates a destabilization that is localized at the mutation site and is undetected with the particular residues monitored.

This study reveals that the early event in the urea-induced unfolding of PrP^C is the dissociation of the β-sheet, and that this is true regardless of the nature of the species studied. This provides experimental support for the hypothesis that β-sheet dissociation is an early and essential event in the PrP^{Sc}-induced misfolding of PrP^C,[24] and that a partial molten globule state ("demiglobule") may serve as a conversion intermediate.[51] That said, the propensity of a prion protein to participate in disease misfolding is not predicted by its global susceptibility to denaturation, because this study shows that the relative stability of the PrP^C proteins is in the following order: hamster ≤ mouse < rabbit < bovine.

■ ASSOCIATED CONTENT

Ⓢ Supporting Information

Stacked plots of the 1D ^1H NMR spectra acquired during the urea denaturation of the three constructs of $shPrP^C$ [shPrP(90−232), shPrP(90−232H), and shPrP(120−232H)] (Figure S1), stacked plots of the 1D ^1H NMR spectra acquired during the urea denaturation of wild-type and S174N $raPrP^C$ (Figure S2), fits of the peak integrals as a function of urea concentration for all constructs that reflect the thermodynamic data presented in Tables 1 and 2 (Figure S3), and urea denaturation of bPrP(121−230) monitored using CD spectroscopy (Figure S4). This material is available free of charge via the Internet at http://pubs.acs.org.

■ AUTHOR INFORMATION

Corresponding Author

*Address: 4-19 Medical Sciences Building, Department of Biochemistry, University of Alberta, Edmonton, AB, Canada T6G 2H7. Phone: (780) 492-5460. Fax: (780) 492-0886. E-mail: brian.sykes@ualberta.ca.

Author Contributions

O.J. and S.C. contributed equally to this work.

Funding

This work was supported by the Alberta Prion Research Institute (funded by Alberta Ingenuity), PrioNet Canada (funded by the Networks of Centres of Excellence Canada Program and the Canadian Institutes of Health Research), and the Ontario Ministry of Health and Long-term Care. O.J. is the recipient of an AHFMR studentship and a Frederick Banting and Charles Best Canada Graduate Doctoral Scholarship from CIHR.

■ ACKNOWLEDGMENTS

We thank Dave Corson and Angela Thiessen for their technical help. We thank the Canadian National High Field NMR Centre (NANUC) for their assistance and providing the 800 MHz NMR facilities.

■ ABBREVIATIONS

NMR, nuclear magnetic resonance; CD, circular dichroism; PrP, prion protein; PrP^{C}, cellular form of PrP; PrP^{Sc}, misfolded form of PrP; bPrP, bovine PrP; shPrP, Syrian hamster PrP; moPrP, mouse PrP; raPrP, rabbit PrP; PDB, Protein Data Bank.

■ REFERENCES

(1) Prusiner, S. B. (1982) Novel proteinaceous infectious particles cause scrapie. *Science 216*, 136−144.

(2) Prusiner, S. B. (1998) Prions. *Proc. Natl. Acad. Sci. U.S.A. 95*, 13363−13383.

(3) Collinge, J. (2001) Prion diseases of humans and animals: Their causes and molecular basis. *Annu. Rev. Neurosci. 24*, 519−550.

(4) Aguzzi, A., Sigurdson, C., and Heikenwaelder, M. (2008) Molecular mechanisms of prion pathogenesis. *Annu. Rev. Pathol. 3*, 11−40.

(5) Caughey, B., and Baron, G. S. (2006) Prions and their partners in crime. *Nature 443*, 803−810.

(6) Weissmann, C. (2004) The state of the prion. *Nat. Rev. Microbiol. 2*, 861−871.

(7) Caughey, B. W., Dong, A., Bhat, K. S., Ernst, D., Hayes, S. F., and Caughey, W. S. (1991) Secondary structure analysis of the scrapie-associated protein PrP 27−30 in water by infrared spectroscopy. *Biochemistry 30*, 7672−7680.

(8) Safar, J., Roller, P. P., Gajdusek, D. C., and Gibbs, C. J. J. (1993) Thermal stability and conformational transitions of scrapie amyloid (prion) protein correlate with infectivity. *Protein Sci. 2*, 2206−2216.

(9) Pan, K. M., Baldwin, M., Nguyen, J., Gasset, M., Serban, A., Groth, D., Mehlhorn, I., Huang, Z., Fletterick, R. J., Cohen, F. E., and Prusiner, S. B. (1993) Conversion of α-helices into β-sheets features in the formation of the scrapie prion proteins. *Proc. Natl. Acad. Sci. U.S.A. 90*, 10962−10966.

(10) Rieger, R., Edenhofer, F., Lasmezas, C. I., and Weiss, S. (1997) The human 37-kDa laminin receptor precursor interacts with the prion protein in eukaryotic cells. *Nat. Med. 3*, 1383−1388.

(11) Telling, G. C., Scott, M., Mastrianni, J., Gabizon, R., Torchia, M., Cohen, F. E., DeArmond, S. J., and Prusiner, S. B. (1995) Prion propagation in mice expressing human and chimeric PrP transgenes implicates the interaction of cellular PrP with another protein. *Cell 83*, 79−90.

(12) Mouillet-Richard, S., Ermonval, M., Chebassier, C., Laplanche, J. L., Lehmann, S., Launay, J. M., and Kellermann, O. (2000) Signal transduction through prion protein. *Science 289*, 1925−1928.

(13) Brown, D. R., Qin, K., Herms, J. W., Madlung, A., Manson, J., Strome, R., Fraser, P. E., Kruck, T., von Bohlen, A., Schulz-Schaeffer, W., Giese, A., Westaway, D., and Kretzschmar, H. (1997) The cellular prion protein binds copper in vivo. *Nature 390*, 684−687.

(14) Riek, R., Hornemann, S., Wider, G., Billeter, M., Glockshuber, R., and Wuthrich, K. (1996) NMR structure of the mouse prion protein domain PrP(121−231). *Nature 382*, 180−182.

(15) Julien, O., Graether, S. P., and Sykes, B. D. (2009) Monitoring prion protein stability by NMR. *J. Toxicol. Environ. Health, Part A 72*, 1069−1074.

(16) DeMarco, M. L., and Daggett, V. (2004) From conversion to aggregation: Protofibril formation of the prion protein. *Proc. Natl. Acad. Sci. U.S.A. 101*, 2293−2298.

(17) DeMarco, M. L., Silveira, J., Caughey, B., and Daggett, V. (2006) Structural properties of prion protein protofibrils and fibrils: An experimental assessment of atomic models. *Biochemistry 45*, 15573−15582.

(18) Wille, H., Michelitsch, M. D., Guenebaut, V., Supattapone, S., Serban, A., Cohen, F. E., Agard, D. A., and Prusiner, S. B. (2002) Structural studies of the scrapie prion protein by electron crystallography. *Proc. Natl. Acad. Sci. U.S.A. 99*, 3563−3568.

(19) Govaerts, C., Wille, H., Prusiner, S. B., and Cohen, F. E. (2004) Evidence for assembly of prions with left-handed β-helices into trimers. *Proc. Natl. Acad. Sci. U.S.A. 101*, 8342−8347.

(20) Wasmer, C., Lange, A., Van Melckebeke, H., Siemer, A. B., Riek, R., and Meier, B. H. (2008) Amyloid fibrils of the HET-s(218−289) prion form a β solenoid with a triangular hydrophobic core. *Science 319*, 1523−1526.

(21) Cobb, N. J., Sonnichsen, F. D., McHaourab, H., and Surewicz, W. K. (2007) Molecular architecture of human prion protein amyloid: A parallel, in-register β-structure. *Proc. Natl. Acad. Sci. U.S.A. 104*, 18946−18951.

(22) Smirnovas, V., Baron, G. S., Offerdahl, D. K., Raymond, G. J., Caughey, B., and Surewicz, W. K. (2011) Structural organization of brain-derived mammalian prions examined by hydrogen-deuterium exchange. *Nat. Struct. Mol. Biol. 18*, 504−506.

(23) Barducci, A., Chelli, R., Procacci, P., Schettino, V., Gervasio, F. L., and Parrinello, M. (2006) Metadynamics simulation of prion protein: β-Structure stability and the early stages of misfolding. *J. Am. Chem. Soc. 128*, 2705−2710.

(24) Paramithiotis, E., Pinard, M., Lawton, T., LaBoissiere, S., Leathers, V. L., Zou, W. Q., Estey, L. A., Lamontagne, J., Lehto, M. T., Kondejewski, L. H., Francoeur, G. P., Papadopoulos, M., Haghighat, A., Spatz, S. J., Head, M., Will, R., Ironside, J., O'Rourke, K., Tonelli, Q., Ledebur, H. C., Chakrabartty, A., and Cashman, N. R. (2003) A prion protein epitope selective for the pathologically misfolded conformation. *Nat. Med. 9*, 893−899.

(25) O'Sullivan, D.B., Jones, C. E., Abdelraheim, S. R., Brazier, M. W., Toms, H., Brown, D. R., and Viles, J. H. (2009) Dynamics of a truncated prion protein, PrP(113−231), from ^{15}N NMR relaxation: Order parameters calculated and slow conformational fluctuations localized to a distinct region. *Protein Sci. 18*, 410−423.

(26) Julien, O., Chatterjee, S., Thiessen, A., Graether, S. P., and Sykes, B. D. (2009) Differential stability of the bovine prion protein upon urea unfolding. *Protein Sci. 18*, 2172−2182.

(27) Barlow, R. M., and Rennie, J. C. (1976) The fate of ME7 scrapie infection in rats, guinea-pigs and rabbits. *Res. Vet. Sci. 21*, 110−111.

(28) Gibbs, C. J. J., and Gajdusek, D. C. (1973) Experimental subacute spongiform virus encephalopathies in primates and other laboratory animals. *Science 182*, 67−68.

(29) Vorberg, I., Groschup, M. H., Pfaff, E., and Priola, S. A. (2003) Multiple amino acid residues within the rabbit prion protein inhibit formation of its abnormal isoform. *J. Virol. 77*, 2003−2009.

(30) Priola, S. A., and Chesebro, B. (1995) A single hamster PrP amino acid blocks conversion to protease-resistant PrP in scrapie-infected mouse neuroblastoma cells. *J. Virol. 69*, 7754−7758.

(31) Castilla, J., Gonzalez-Romero, D., Saa, P., Morales, R., De Castro, J., and Soto, C. (2008) Crossing the species barrier by PrP(Sc) replication in vitro generates unique infectious prions. *Cell 134*, 757−768.

(32) Barria, M. A., Telling, G. C., Gambetti, P., Mastrianni, J. A., and Soto, C. (2011) Generation of a New Form of Human PrPSc in Vitro by Interspecies Transmission from Cervid Prions. *J. Biol. Chem. 286*, 7490−7495.

(33) Baskakov, I. V., Legname, G., Gryczynski, Z., and Prusiner, S. B. (2004) The peculiar nature of unfolding of the human prion protein. *Protein Sci. 13*, 586−595.

(34) Baskakov, I.V., Legname, G., Baldwin, M. A., Prusiner, S. B., and Cohen, F. E. (2002) Pathway complexity of prion protein assembly into amyloid. *J. Biol. Chem. 277*, 21140−21148.

(35) Zahn, R., von Schroetter, C., and Wuthrich, K. (1997) Human prion proteins expressed in *Escherichia coli* and purified by high-affinity column refolding. *FEBS Lett. 417*, 400−404.

(36) Baryshnikova, O. K., Williams, T. C., and Sykes, B. D. (2008) Internal pH indicators for biomolecular NMR. *J. Biomol. NMR 41*, 5−7.

(37) Khan, M. Q., Sweeting, B., Mulligan, V. K., Arslan, P. E., Cashman, N. R., Pai, E. F., and Chakrabartty, A. (2010) Prion disease susceptibility is affected by β-structure folding propensity and local side-chain interactions in PrP. *Proc. Natl. Acad. Sci. U.S.A. 107*, 19808−19813.

(38) Greene, R. F. J., and Pace, C. N. (1974) Urea and guanidine hydrochloride denaturation of ribonuclease, lysozyme, α-chymotrypsin, and β-lactoglobulin. *J. Biol. Chem. 249*, 5388−5393.

(39) Pace, C. N. (1986) Determination and analysis of urea and guanidine hydrochloride denaturation curves. *Methods Enzymol. 131*, 266−280.

(40) Hornemann, S., Schorn, C., and Wuthrich, K. (2004) NMR structure of the bovine prion protein isolated from healthy calf brains. *EMBO Rep. 5*, 1159−1164.

(41) Chakroun, N., Prigent, S., Dreiss, C. A., Noinville, S., Chapuis, C., Fraternali, F., and Rezaei, H. (2010) The oligomerization properties of prion protein are restricted to the H2H3 domain. *FASEB J. 24*, 3222−3231.

(42) Adrover, M., Pauwels, K., Prigent, S., de Chiara, C., Xu, Z., Chapuis, C., Pastore, A., and Rezaei, H. (2010) Prion fibrillization is mediated by a native structural element that comprises helices H2 and H3. *J. Biol. Chem. 285*, 21004−21012.

(43) Gossert, A.D., Bonjour, S., Lysek, D. A., Fiorito, F., and Wuthrich, K. (2005) Prion protein NMR structures of elk and of mouse/elk hybrids. *Proc. Natl. Acad. Sci. U.S.A. 102*, 646−650.

(44) Soto, C. (2009) Constraining the loop, releasing prion infectivity. *Proc. Natl. Acad. Sci. U.S.A. 106*, 10−11.

(45) Deleault, N. R., Harris, B. T., Rees, J. R., and Supattapone, S. (2007) Formation of native prions from minimal components in vitro. *Proc. Natl. Acad. Sci. U.S.A. 104*, 9741−9746.

(46) Wang, F., Wang, X., Yuan, C. G., and Ma, J. (2010) Generating a prion with bacterially expressed recombinant prion protein. *Science 327*, 1132−1135.

(47) Blinov, N., Berjanskii, M., Wishart, D. S., and Stepanova, M. (2009) Structural domains and main-chain flexibility in prion proteins. *Biochemistry 48*, 1488−1497.

(48) Guest, W. C., Cashman, N. R., and Plotkin, S. S. (2010) Electrostatics in the stability and misfolding of the prion protein: Salt bridges, self energy, and solvation. *Biochem. Cell Biol. 88*, 371−381.

(49) Zhang, J. (2010) Studies on the structural stability of rabbit prion probed by molecular dynamics simulations of its wild-type and mutants. *J. Theor. Biol. 264*, 119−122.

(50) Wen, Y., Li, J., Yao, W., Xiong, M., Hong, J., Peng, Y., Xiao, G., and Lin, D. (2010) Unique structural characteristics of the rabbit prion protein. *J. Biol. Chem. 285*, 31682−31693.

(51) Li, L., Guest, W., Huang, A., Plotkin, S. S., and Cashman, N. R. (2009) Immunological mimicry of PrPC-PrPSc interactions: Antibody-induced PrP misfolding. *Protein Eng., Des. Sel. 22*, 523−529.